PHYSICAL REVIEW A VOLUME 51, NUMBER 3 MARCH 1995

Laser-induced collisional avalanche in atomic cesium

A. Lenef, D. Kreysar, K. Obermyer, and S. C. Rand
Division of Applied Physics, 1049 Randall Laboratory, University of Michigan, Ann Arbor, Michigan 48109-1120
(Received 3 March 1994)

Radiation tuned to an *excited-state transition* in dense cesium vapor results in the appearance of induced absorption and fluorescence after delays of up to 5 s, an observation ascribed to a chain reaction of resonant binary collisions initiated by the incident light. Our results occur in a nonlinear regime characterized by high collision rates, which are variable in a controlled fashion at *constant* vapor density.

PACS number(s): 34.30.+h, 33.50.−j, 33.80.−b, 42.50.Fx

Collisional interactions of Rydberg states in atomic vapors have been the subject of intense inquiry in the past. At low excited-state densities, the velocity [1] and spin [2] dependence of associative ionization [3] have been carefully studied, and cross sections for fine-structure-changing collisions [4,5], excitation transfer, and "energy-pooling" [6–8] have been examined. Intriguingly large cross sections ($\sim 10^{-14}$ cm^2) have been reported for some near-resonant collisional processes, but have fostered little research in dense vapors for the simple reason that such systems are optically opaque on ground-state transitions. In this paper we report what we believe to be the first observation of a nonlinear process involving resonant collisions in dense cesium vapor, namely a laser-induced collisional avalanche (LICA), in a regime characterized by exceptionally high collision rates and excited-state density with minimal ionization. The avalanche process is accompanied by delays in the appearance of excited-state fluorescence as long as several seconds, and induces resonant nonlinear optical response with a threshold in spectral regions of transparency. This process is expected to furnish a tool for the study and control of atomic collisions at excited-state densities high enough to permit direct observations of delocalized, nonlinear dynamics dominated (rather than merely perturbed) by collisional interactions. For example, it should permit studies of collisional shift contributions to the Lorentz local field in a particularly direct manner, by providing a means of varying collision rate at *constant* vapor density. Also, suppression of LICA processes at particular optical field strengths may serve as a useful signature of the as yet unobserved electric magic-angle effect [9]. Furthermore, we point out that avalanche phenomena hold implications for intrinsically bistable dynamics of dressed collisional interactions of ultracold atoms in traps.

The excitation transfer collision $Cs^*(6D_{3/2})+Cs(6S_{1/2}) \rightarrow Cs^*(6P)+Cs^*(6P)$ indicated in the inset of Fig. 1 is resonant for colliding atoms that make dipole-allowed electronic transitions with an energy defect $\Delta E = |\Delta E_1 - \Delta E_2| < k_B T$. The role of incident radiation in the phenomenon described here is to promote excited ($6p$) "seed" atoms to a higher ($6d$) state (through intermediate state $8s$) from which an avalanche of excited-state population is possible via the resonant collision process. It was noted some years ago [10] that at densities above 10^{15} cm^{-3} in atomic cesium, light tuned to the atomic $6p$-$6d$ excited-state absorption (ESA) transition at 876.4 nm weakly populated the $6p$ state via the dissociative Cs_2 $X\,^3\Sigma_u^+ - A\,^3\Pi_g$ transition [11], thereby initiating collisional excitation transfer between $6d$ and ground-state atoms. Each resonant $6s$-$6d$ collision tends to produce two $6p$ atoms. An enhanced $6p$ population causes increased absorption, tending to enhance the rate of excited-state collisions further. In the earlier work, the sudden appearance of a laser-produced plasma was reported at 6 kW/cm^2 when the density reached approximately 10^{16} cm^{-3}, coincident with a calculated threshold for runaway growth of $6p$ population. It was concluded that the collisional "critical" reaction caused plasma formation. However, our measurements have revealed in a dramatic way that a runaway or "avalanche" collision regime is accessible in cesium well below the threshold for plasma formation, and that the high rate of excited-state dipolar interactions induced under these conditions opens the door to nonlinear

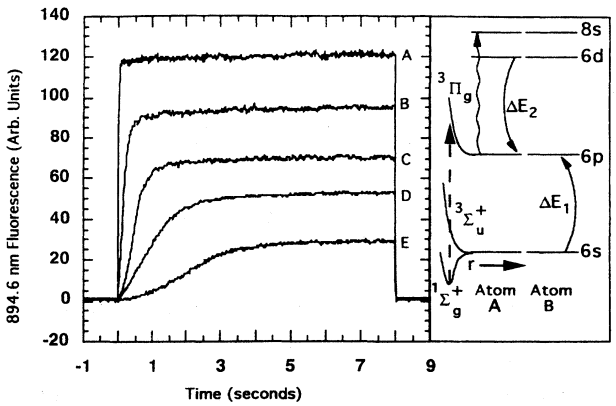

FIG. 1. Fluorescence intensity on the $6p\,^2P_{1/2}$–$6s\,^2S_{1/2}$ transition at 894.6 nm versus time in Cs (density 5×10^{16} cm^{-3}). The sample was excited on the $6p$-$8s$ *excited-state transition* at 761.1 nm for 8 s, with a collimated beam of $1/e^2$ diameter $\phi=3$ mm at powers of 255, 145, 115, 45, and 38 mW (traces A through E). Individual curves were scaled for convenient comparison. Inset: energy levels of two cesium atoms (A and B) and schematic of the laser-induced collisional avalanche (LICA) process. Asymptotic levels of colliding atoms A and B are shown on the right and the molecular potential indicated at small internuclear separations r on the left. Molecular "seed" absorption by a predissociative dimer containing atom A (dashed vertical arrow) is followed by excited-state absorption (straight arrow) and relaxation to the $6d$ state. Curved arrows show the subsequent collision-induced transition between a $6d$ atom (A) and a ground-state atom (B).

collision studies and several applications in dense media.

Conditions required to reach the avalanche collision regime can be estimated by considering excited-state population dynamics that incorporate optical ESA and the binary collisional relaxation of Fig. 1. Density matrix equations of motion for a four-level model obtained from the Liouville equation are

$$\dot{\rho}_{11}=-\lambda_{12}(\rho_{11}-\rho_{22})+\gamma_2\rho_{22}+\gamma_{31}\rho_{33}+\gamma_{41}\rho_{44}-\sigma v\rho_{11}\rho_{33}+\sigma v\rho_{22}^2, \quad (1)$$

$$\dot{\rho}_{22}=1/i\hbar\,(V_{24}\rho_{42}-\rho_{24}V_{42})+\lambda_{12}(\rho_{11}-\rho_{22})-\gamma_2\rho_{22}+\gamma_{32}\rho_{33}+\gamma_{42}\rho_{44}+2\sigma v\rho_{11}\rho_{33}-2\sigma v\rho_{22}^2, \quad (2)$$

$$\dot{\rho}_{33}=-\gamma_3\rho_{33}+\gamma_{43}\rho_{44}-\sigma v\rho_{11}\rho_{33}+\sigma v\rho_{22}^2, \quad (3)$$

$$\dot{\rho}_{44}=1/i\hbar\,(V_{42}\rho_{24}-\rho_{42}V_{24})-\gamma_4\rho_{44}. \quad (4)$$

Here the correspondence with Cs levels is $1\leftrightarrow 6s$, $2\leftrightarrow 6p$, $3\leftrightarrow 6d$, and $4\leftrightarrow 8s$. Optical coherence is governed by the additional coupled equation

$$\dot{\rho}_{24}=i\omega_0\rho_{24}+V_{24}/i\hbar\,(\rho_{44}-\rho_{22})-\Gamma_{24}\rho_{24}. \quad (5)$$

The optical interaction is represented by $V=-\hbar[\Omega\exp(i\phi)+\text{c.c.}]$, where $\Omega=\mu E/2\hbar$, $\omega_0=(H_{44}-H_{22})/\hbar$, and $\phi=\omega t-kx$. Here λ, γ, and Γ are rates for incoherent pumping, incoherent decay, and coherent decay, respectively. σ is the cross section for the collisional relaxation of Fig. 1, and v is the atomic velocity.

In the rotating-wave approximation, the steady-state solution for population in the first excited state (predicated on there being a finite seed rate λ_{12}) is found to be

$$\rho_{22}=\frac{-[\alpha(a_2a_3+a_1a_4)+\gamma_3a_4+\gamma_{43}a_5]\pm\sqrt{[\alpha(a_2a_3+a_1a_4)+a_4\gamma_3+a_5\gamma_{43}]^2+4\alpha[1-a_2a_4][\alpha a_1a_3+a_3\gamma_3]}}{2\alpha(1-a_2a_4)}.$$

For convenience a collisional parameter $\alpha=\sigma V$ has been introduced. Explicit expressions for the coefficients $a_i(i=1,\ldots,5)$ are

$$a_1=(\gamma_3+\gamma_{31})/(\lambda_{12}+\gamma_3+\gamma_{31}),$$

$$a_2=\frac{-\gamma_2-(\gamma_{41}-\gamma_{43})a_5+(\gamma_3+\gamma_{31})(1+a_5)}{\lambda_{12}+\gamma_3+\gamma_{31}},$$

$$a_3=\lambda_{12}/(\lambda_{12}+\gamma_3+\gamma_{31}),$$

$$a_4=\frac{\lambda_{12}(1+a_5)+\gamma_2+a_5(\gamma_{41}-\gamma_{43})}{\lambda_{12}+\gamma_3+\gamma_{31}},$$

$$a_5=\frac{2|\Omega|^2\Gamma_{24}/(\Delta^2+\Gamma_{24}^2)}{\gamma_4+2|\Omega|^2\Gamma_{24}/(\Delta^2+\Gamma_{24}^2)}.$$

The solution for the optical coherence as a function of detuning $\Delta=\omega-\omega_0$ is simply $\rho_{24}=\Omega(\rho_{44}-\rho_{22})/(\Delta-i\Gamma_{24})$, with $\rho_{44}=a_5\rho_{22}$.

Solutions of Eqs. (1)–(5) predict striking features of collisional interactions driven by excited-state absorption of light. For instance, in the regime in which the collision-induced decay rate of state 3 exceeds the state-2 decay rate ($\rho_{11}\rho_{33}\sigma v>\rho_{22}/\tau_2$), a threshold for excited-state absorption is reached. This threshold is a unique characteristic of the collisional avalanche. Assuming optical saturation, a Maxwellian distribution of velocities, and a cross section of $\sigma=1.5\times10^{-14}$ cm^2 [6], the avalanche condition can be met in cesium above 580 K, or a density of 4×10^{16} cm^{-3}. The model indicates that the nonlinear absorption is relatively insensitive to the "seeding" process, which, through weak excitation overlap with ground-state absorptions or thermal excitation or other means, provides an initial state-2 population that grows until the collision rate is limited by incident photon flux. Long delays are predicted in the appearance of avalanche fluorescence after excitation is switched on. These effects vanish ($\rho_{22}=\rho_{24}=0$) if the collisional interaction vanishes ($\sigma=0$).

In our experiments, a continuous-wave Ti:sapphire laser was tuned to the $6p\,^2P_{1/2}$–$8s\,^2S_{1/2}$ ESA transition at 761.1 nm. At this wavelength dense Cs vapor is transparent, since the thermal $6p$ population is negligible. Sample chambers were simple quartz cells of dimensions $t\times1\times4$ cm^3 ($t=0.2,0.5,1$), with in-line reservoirs containing vacuum-distilled high-purity (99.99%) solid cesium. A copper shroud wrapped with heating tape and glass wool was used to heat the assembly to the range 550–650 K. Temperature was monitored using thermocouples on the quartz envelope, near the reservoir and optical axis. Auxiliary heaters in the vicinity of the optical ports maintained a small temperature gradient to prevent condensation on the windows. Vapor pressures were estimated from measured reservoir temperatures [12].

Time-resolved fluorescence emitted by $6p\,^2P_{1/2}$ atoms is shown in Figs. 1 and 2. Since fluorescence intensity is directly proportional to the excited-state occupation, these results clearly indicate that $6p$ population rises abruptly, long after light is introduced into the cell. Under conditions of weakest illumination the fluorescence delay extends to approximately 5 s, a time scale much longer than that of any electronic decay process of Cs atoms or molecules. For instance, the $6p$ radiative decay time is 35 ns [13]. Although radiation trapping is expected to extend the $6p\,^2P_{1/2}$ lifetime to 39 μs [10,14], explanations of fluorescence delays on the time scale of seconds in terms of radiation trapping may be dismissed by the simple observation that excited-state emission disappears immediately when pumping is terminated (trailing edge in Fig. 2). Moreover, similar delays are observed in $6d\,^2D_{3/2}$ emission, which is not trapped.

While the two-parameter fit of Fig. 2 required an effective lifetime ($\tau_3=1$ μs) somewhat longer than the $6d$ lifetime

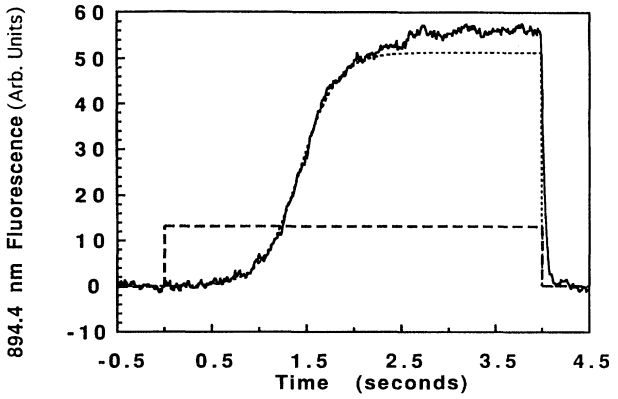

FIG. 2. Comparison of calculated and observed fluorescence intensity on the $6p\ ^2P_{1/2}$–$6s\ ^2S_{1/2}$ transition at 894.6 nm (lower curve) versus time. The dashed curve shows the rectangular envelope of the incident pulse and the solid line is data. The dotted curve gives a calculation based on Eqs. (1)–(5) and an effective lifetime $\tau_2 = 100\ \mu$s. Other parameters were $\gamma_{31} = 0$, $\gamma_{43}^{-1} = 50$ ns, $\gamma_{41} = 0$, $\gamma_4^{-1} = \gamma_{42}^{-1} = 95$ ns, and $v = 4.4 \times 10^4$ cm/s. The optical intensity and Cs density assumed their experimental values ($I = 0.05$ W/cm^2, $\rho = 8 \times 10^{16}$ cm^{-3}, respectively). The only adjustable parameters were $\gamma_3^{-1} = \gamma_{32}^{-1} = 1.0\ \mu$s and $\lambda_{12} = 1.8 \times 10^{-8}$ s^{-1}. The variation in response versus intensity (Fig. 1) was well reproduced for fixed parameters.

(60 ns) reported under similar experimental conditions [15], the data showed that, as intensity increased, fluorescent delays shortened and the curves evolved from sigmoid to saturated exponential, in excellent agreement with numerical solutions of Eqs. (1)–(5). The extended d state lifetime in the fit may simply reflect our neglect of the $5d$ and other intermediate states, which do not participate in cross relaxation but have long radiative lifetimes [16] capable of greatly reducing the effective excited-state saturation intensity. Simulations also revealed that if the trapped $6p$ lifetime was assigned values on the order of milliseconds (greater than the calculated 39 μs), avalanche delays exhibited little sensitivity to intensity or vapor density variations. While perhaps surprising for a "critical" reaction, this too was in qualitative accord with the large intensity range over which substantial delays were observed (Fig. 1).

These unusual dynamics were induced by narrow-band excitation at 761.1 nm, the wavelength of the $6p\ ^2P_{1/2}$–$8s\ ^2S_{1/2}$ atomic Cs (ESA) transition. $6d$ fluorescence (Fig. 3) can be excited only at this wavelength since atomic excited-state absorption is necessary to reach such a level, lying at nearly twice the photon energy. On the other hand, $6p$ population arises quite differently. Cesium dimer absorption in the overlapping $X\ ^1\Sigma_g^+$–$B\ ^1\Pi_u$ band at 766.7 nm furnishes $6p$ population by predissociation [17], and excited-state collisions also promote $6s$ atoms to $6p$ following absorption on the atomic ESA transition. Consequently the excitation of $6p$ fluorescence reflects both these contributions in a broad spectrum containing molecular vibrational structure (Fig. 3 inset).

For measurements of fluorescence delays, optical intensity was always at least a factor of 10 below the threshold value that generated a visible plasma, rendering ionic emission intensity weak compared to atomic and molecular transitions (Fig. 4). In contrast to earlier work [18], no transmission changes ($<0.5\%$) due to plasma absorption were

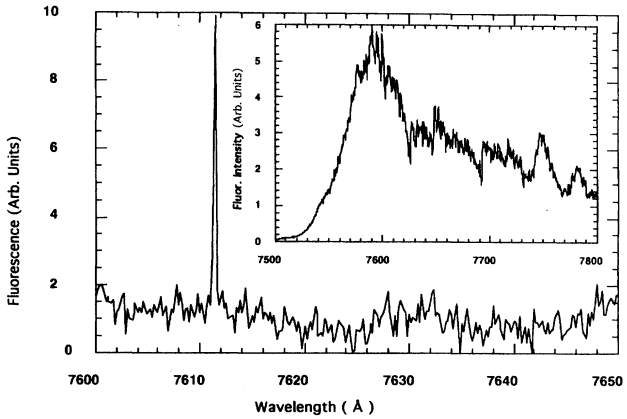

FIG. 3. Excitation spectra of fluorescence observed at $\lambda = 876.4$ nm ($6d\ ^2D_{3/2} \rightarrow 6p\ ^2P_{1/2}$) and (inset) $\lambda = 894.6$ nm ($6p\ ^2P_{1/2} \rightarrow 6s\ ^2S_{1/2}$).

observed under these conditions. Nevertheless, broad emission bands observed in spectral regions around 595 nm, 712 nm, and beyond 750 nm *above plasma threshold* (Fig. 4 inset) were studied to rule out delay mechanisms ascribable to ionic dynamics. For instance, the Cs^{3+} dissociative recombination lifetime was measured directly without electrodes in the cell by tuning to the wavelength 712 nm [19]. This yielded $\tau_{ion} < 10\ \mu$s (trailing edge decays in Fig. 5). In this way, recombination on this and other lines was shown to be much faster than, and unrelated to, the avalanche dynamics of Fig. 1. The excited-state collision rate, proportional to $6d\ ^2D_{3/2}$ population, was also shown to depend on input intensity above avalanche threshold (Fig. 6).

In our analysis, subtle dynamic correlations due to ground-state depletion, delocalization of wave functions, velocity averaging, and fine and hyperfine structure were ignored. More detailed density-matrix treatments might address such refinements. For example, as more and more atoms participate in correlated dynamics, collisional decay

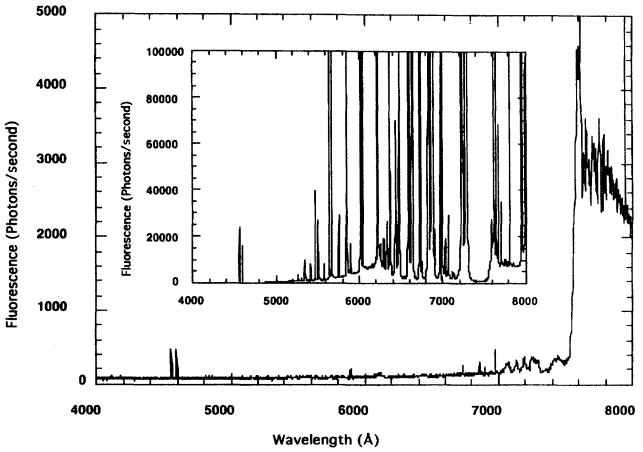

FIG. 4. Fluorescent emissions in the visible spectral region excited by irradiation at 761.1 nm. For the main trace $I = 10$ W/cm^2, revealing only neutral-atom and dimer features. For the inset, $I = 200$ W/cm^2 and plasma recombination continua emerge due to increased laser intensity, dwarfing the 455-nm Cs resonance line.

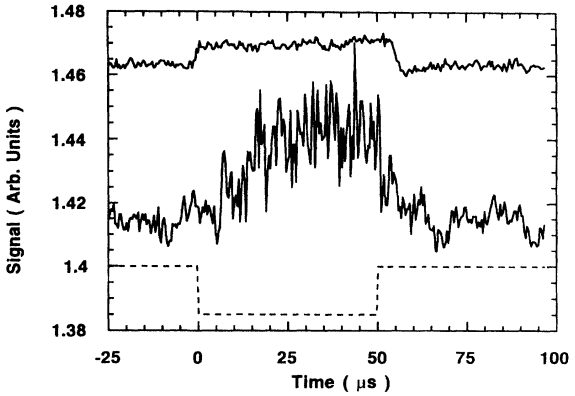

FIG. 5. Time-resolved plasma emission. The lowest trace shows the 50-μs envelope of the excitation pulse (inverted). The middle trace, recorded at $\lambda = 712$ nm gives the Cs_3^+ dissociative recombination intensity resulting from the reaction $Cs_3^+ + e \rightarrow Cs_2 + Cs$ followed by $Cs_2 \rightarrow 2Cs + h\nu$ [3,15]. The upper trace is a similar measurement of continuum emission at $\lambda = 595$ nm.

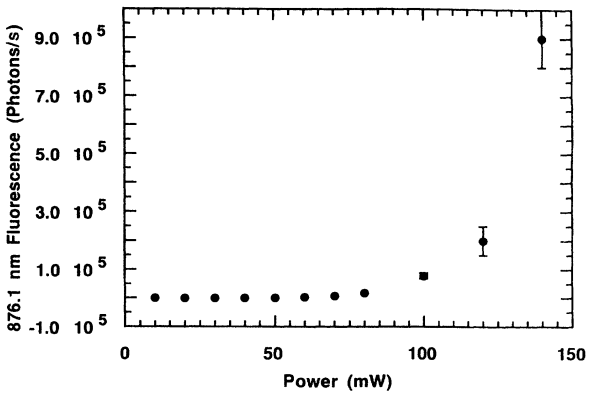

FIG. 6. Fluorescence intensity at $\lambda = 876.4$ nm versus power, showing threshold behavior and dependence of laser-induced collision rate on incident light intensity.

rates should deviate from simple proportionality to occupation probabilities of independent atoms. However, the simple picture presented here satisfactorily explains the basic features of ESA with a threshold and delayed response in atomic cesium.

In summary, we have observed the delayed promotion of ground-state Cs atoms to the $6p$ state in an avalanche of electronic excitation attributed to light-induced, collisional processes. The time scale of the longest delays was set by a critical balance of excitation and decay rates. $6d$ population and hence the excited-state collision rate were varied optically at constant density in the avalanche regime, furnishing a method for identifying collisional contributions to dephasing processes or collisional shifts [20] in nonlinear interactions. Radiation trapping reduces the optical intensities needed to observe the avalanche, but is unrelated to its mechanism. The LICA process may prove to be of importance for ultracold cesium atoms despite the low densities encountered in present generation atom traps, because, even for velocities approaching zero, α should still diverge. Additionally, intrinsic bistability due to excited-state interactions similar to those discussed here has been observed recently [21] and may be of considerable importance in the nonclassical collision regime of ultracold atoms in dense systems. Finally, because avalanche-induced absorption in Cs overlaps diode laser wavelengths, we note that applications to compact far infrared gas lasers pumped by avalanche absorption and operating on previously reported Rydberg laser transitions [22] may be possible.

We thank Coherent Radiation for the loan of a MIRA sapphire laser, K. Schepler for assisting with preliminary work, L. Krause and M. Allegrini for useful discussions, J. Zorn for samples, and P. Berman for reading the manuscript. A.L. and K.O. thank the U.S. Department of Education and the National Physical Science Consortium, respectively, for financial support. The authors gratefully acknowledge partial support of this research by the U.S. Air Force Office of Scientific Research.

[1] M.-X. Wang *et al.*, Phys. Rev. A **32**, 681 (1985).
[2] M.-X. Wang *et al.*, Phys. Rev. A **35**, 934 (1987).
[3] W. C. Stwalley and J. T. Bahns, Laser Part. Beams **11**, 185 (1993).
[4] A. C. Tam *et al.*, Phys. Rev. A **17**, 1862 (1978).
[5] P. W. Arcuni *et al.*, Phys. Rev. A **41**, 2398 (1990).
[6] M. Allegrini *et al.*, J. Phys. (Paris) Colloq. **46**, C1-61 (1985).
[7] A. Kopystynska and L. Moi, Phys. Rep. **92**, 135 (1982).
[8] H. G. C. Werij *et al.*, Phys. Rev. A **43**, 2237 (1991).
[9] J. F. Lam and S. C. Rand, Phys. Rev. A **35**, 2164 (1987).
[10] T. Yabuzaki *et al.*, Opt. Commun. **24**, 305 (1978).
[11] F. W. Loomis and P. Kusch, Phys. Rev. **46**, 292 (1934).
[12] J. B. Taylor and I. Langmuir, Phys. Rev. **51**, 753 (1937).
[13] O. S. Heavens, J. Opt. Soc. Am. **51**, 1058 (1969).
[14] T. Holstein, Phys. Rev. **83**, 1159 (1951); C. L. Chen and A. V. Phelps, *ibid.* **173**, 62 (1968); A. M. Akul'shin *et al.*, Pis'ma Zh. Eksp. Teor. Fiz. **36**, 247 (1982) [JETP Lett. **36**, 303 (1982)].
[15] A. R. Radzig and B. M. Smirnov, *Reference Data on Atoms, Molecules and Ions* (Springer-Verlag, Berlin, 1985), pp. 228 and 245.
[16] A. Sasso *et al.*, Phys. Rev. A **45**, 1670 (1992).
[17] P. Kusch and M. M. Hessel, J. Mol. Spectrosc. **32**, 181 (1969).
[18] P. Verkerk and G. Grynberg, Europhys. Lett. **6**, 31 (1988); A. Tam and W. Happer, Opt. Commun. **21**, 403 (1977).
[19] W.-T. Luh *et al.*, J. Chem. Phys. **88**, 2235 (1988).
[20] J. J. Maki *et al.*, Phys. Rev. Lett. **67**, 972 (1991).
[21] M. Hehlen *et al.*, Phys. Rev. Lett. **73**, 1104 (1994).
[22] S. Jacobs *et al.*, Phys. Rev. Lett. **7**, 415 (1961); P. Rabinowitz *et al.*, Appl. Opt. **1**, 513 (1962).